ЖЭТФ, 2004, том 126, вып. 4 (10), стр. 1006–1020 

# BILAYER MEMBRANE IN CONFINED GEOMETRY: INTERLAYER SLIDE AND ENTROPIC REPULSION

***S. V. Baoukina*[*], *S. I. Mukhin*[**]**

*Moscow State Institute for Steel and Alloys (Technological University)*
*119049, Moscow, Russia*

Submitted 28 April 2004

We derive the free energy functional of a bilayer lipid membrane from the first principles of elasticity theory. The model explicitly includes position-dependent mutual slide of monolayers and bending deformation. Our free energy functional of a liquid-crystalline membrane allows for incompressibility of the membrane and vanishing of the in-plane shear modulus and obeys reflectional and rotational symmetries of the flat bilayer. Interlayer slide at the mid-plane of the membrane results in a local difference of the surface densities of monolayers. The slide amplitude directly enters the free energy via the strain tensor. For small bending deformations, the ratio between the bending modulus and the area compression coefficient, $K_b/K_A$, is proportional to the square of monolayer thickness $h$. Using the functional, we perform self-consistent calculation of the entropic potential acting on a bilayer between parallel confining walls separated by distance $2d$. We find that at the minimum of the confining potential, the temperature-dependent curvature $\alpha \propto T^2/K_b d^4$ is enhanced four times for a bilayer with slide as compared to a unit bilayer. We also calculate viscous modes of a bilayer membrane between confining walls. We investigate pure bending of the membrane, which is decoupled from area dilation at small amplitudes. Three sources of viscous dissipation are considered: water and membrane viscosities and interlayer drag. The dispersion relation gives two branches $\omega_{1,2}(q)$.

PACS: 68.15.+e, 68.60.-Bs, 87.16.Dg

## 1. INTRODUCTION

Cell membrane is characterized by complex structural and dynamical properties [1–4]. Theoretical modeling and description of lipid membranes are of great fundamental and practical interest and have a sufficiently long history. The phenomenological model introduced in [5] treated a lipid membrane as a single sheet with bending rigidity and spontaneous curvature. This model was later used for calculation of the frequency spectrum of the membrane in water solution [6] and for investigation of entropic interactions of membranes in multilayer systems [7]. The bilayer structure of a lipid membrane was analyzed in [3, 8], where the dynamic coupling between the monolayers and the interlayer slide was considered. The frequency spectrum of a membrane in the bulk water was recalculated in [9] with the coupling between local curvature and local densities of lipids within the monolayers taken into account. Afterwards, viscous modes of a bilayer adhering to a substrate were found in [10] using the density-difference model [9], supplemented with a binding potential [11].

In this paper, we derive a new free energy functional of a bilayer membrane with interlayer slide. The interlayer slide function, membrane stretching and bending amplitude directly enter the strain tensor of the membrane. Our functional is a generalization of the density-difference model used in [9, 10]. In our model, two lateral deformation fields (interlayer slide and stretching) generate the change in the local density and the density difference of monolayers that were used in the free energy functional in [9, 10]. But unlike in [9, 10], we do not require the presence of neutral surfaces in each monolayer in the general case. As a step towards understanding intermembrane interactions, we study dynamics of a bilayer membrane in water solution confined between parallel walls. The effect of confinement is modeled by the entropic potential [12].

This paper is organized as follows. In Sec. 2, we

[*]E-mail: svt_lana19@yahoo.com
[**]E-mail: sergeimoscow@online.ru

introduce an anisotropic elastic moduli tensor, initially containing 21 independent components. The reflection and rotation symmetries of the flat bilayer reduce the number of components to 5. Next, we impose the zero shear stress modulus and incompressibility constraint. We restrict ourselves to the case of small bending deformations and exclude the corresponding strain and elastic tensor components. Thus, the number of independent components of the elastic tensor in the free energy functional is reduced to two. The derived free energy functional of a bilayer membrane contains three fields describing area dilation and bending deformation coupled to interlayer slide.

In Sec. 3, a parabolic entropic potential acting on the membrane between confining walls is introduced. We self-consistently calculate the curvature of the confining potential at its minimum for a bilayer with slide and for a unit bilayer. Using our model, we analytically derive the four-time decrease in bending rigidity due to interlayer slide.

In Sec. 4, we use the derived functional to study dynamical properties and dissipative mechanisms of the bilayer membrane in water solution confined between parallel walls. We investigate only pure bending deformations of the membrane (zero total lateral stretching), which decouple from area dilation. The velocity field in the surrounding water is found by solving Stokes equations for incompressible fluid. Fluid velocity vanishes at the walls. Equations of motion are determined as force balance conditions on the membrane surfaces with inertial effects neglected. Three sources of dissipation are included into dynamic equations: water and membrane viscosities and interlayer drag.

In Sec. 5, we discuss limitations and possible improvements of our model and correspondence with earlier results [10]. In Appendix A, static behavior of a membrane in the axially symmetric case is studied. Analytic solutions are obtained for a circular membrane bent by external pressure. Membrane bending, interlayer slide, and lateral stress distribution are found as functions of pressure across the membrane. In Appendix B, we rederive the dispersion relation [9] for a membrane in the bulk water solution using our free energy functional.

## 2. FREE ENERGY FUNCTIONAL

The free energy density of an anisotropic medium can be written to the lowest order in the elastic strain tensor as [13, 14]

$$F = \frac{1}{2}\lambda_{iklm} u_{ik} u_{lm}, \qquad (1)$$

where summation over the repeated indices $i$, $k$, $l$, $m$ is performed. The indices $i$, $k$, $l$, $m$ take values 1, 2, 3, labeling the respective space axes $x$, $y$, $z$; $u_{ik}$ is the strain tensor, and $\lambda_{iklm}$ is the elastic (modulus) tensor. By definition, the elastic tensor is symmetric under the transpositions $i \leftrightarrow k$, $l \leftrightarrow m$, and $i, k \leftrightarrow l, m$,

$$\lambda_{iklm} = \lambda_{kilm} = \lambda_{ikml} = \lambda_{lmik},$$

and has 21 independent coefficients.

With (1), the (symmetric) stress tensor $\sigma_{ik}$ is defined as

$$\sigma_{ik} = \frac{\partial F}{\partial u_{ik}} = \lambda_{iklm} u_{lm}. \qquad (2)$$

In a symmetric medium, there is a correlation between different components $\lambda_{iklm}$, and the number of independent elements of the elastic modulus tensor is reduced.

We introduce a Cartesian coordinate system with the $z$ axis perpendicular to the unperturbed (flat) membrane plane and with the monolayer interface (i.e., the bilayer mid-plane) positioned in the $xy$ plane (at $z = 0$). The membrane thickness is equal to $2h$, and the flat membrane is modeled as a thin bilayer plate bounded by the $z = -h$ and $z = h$ planes with in-plane linear dimension $R \gg 2h$. The $xy$ plane is a plane of reflection symmetry. This implies that the free energy must be invariant under the transformation $x \to x$, $y \to y$, $z \to -z$. Therefore, all the components $\lambda_{iklm}$ with an odd number of $z$ indices are equal to zero [10]. The membrane can be considered laterally isotropic. Then the $z$ axis is an axis of rotational symmetry. The expression for the elastic energy density $F$ then becomes [11]

$$\begin{aligned} F = {} & \frac{1}{2}\lambda_{xxxx}(u_{xx}^2 + u_{yy}^2) + \frac{1}{2}\lambda_{zzzz} u_{zz}^2 + \\ & + \lambda_{xxyy} u_{xx} u_{yy} + (\lambda_{xxxx} - \lambda_{xxyy}) u_{xy}^2 + \\ & + \lambda_{xxzz}(u_{xx} u_{zz} + u_{yy} u_{zz}) + 2\lambda_{xzxz}(u_{xz}^2 + u_{yz}^2). \end{aligned} \qquad (3)$$

Assuming that the membrane is in liquid state, we require that the in-plane shear modulus (the coefficient in front of $u_{xy}^2$) vanishes, and thus obtain

$$\lambda_{xxxx} = \lambda_{xxyy}.$$

Hence, expression (3) further simplifies and acquires the form

$$\begin{aligned} F = {} & \frac{1}{2}\lambda_{xxxx}(u_{xx} + u_{yy})^2 + \frac{1}{2}\lambda_{zzzz} u_{zz}^2 + \\ & + \lambda_{xxzz}(u_{xx} u_{zz} + u_{yy} u_{zz}) + 2\lambda_{xzxz}(u_{xz}^2 + u_{yz}^2). \end{aligned} \qquad (4)$$

Let an external force applied perpendicular to the membrane plane induce a small bending deformation

along the $z$ axis. Allowing for a typical experimental situation, we consider a thin membrane with the ratio of its thickness $2h$ to the lateral linear dimension (effective radius) $R$ of the order $10^{-3}$. Hence, we neglect the applied external stresses on the top and bottom membrane surfaces compared to the internal lateral stresses in it. Due to the smallness of the membrane thickness, zero stresses on the surface also vanish in the bulk of the membrane. We therefore impose the condition usually implied for the thin plates [13],

$$\sigma_{xz}(\mathbf{r}) = \sigma_{yz}(\mathbf{r}) = \sigma_{zz}(\mathbf{r}) \equiv 0, \tag{5}$$

where $\mathbf{r}$ spans the membrane bulk. This condition is justified by the fact that small external pressure normal to a thin membrane induces relatively high lateral stresses in it [13]. Indeed, we show in Appendix A that the ratio of the normal stress to the lateral stress is of the order $(h/R)^2$. In accordance with (2) and (4), the $z$-components (5) of the stress tensor are related to the strain tensor components as

$$\sigma_{xz} = 4\lambda_{xzxz}u_{xz}, \quad \sigma_{yz} = 4\lambda_{yzyz}u_{yz}, \tag{6}$$

$$\sigma_{zz} = \lambda_{xxzz}(u_{xx} + u_{yy}) + \lambda_{zzzz}u_{zz}. \tag{7}$$

Combining relations (5) and (7), we find

$$u_{zz} = -\frac{\lambda_{xxzz}}{\lambda_{zzzz}}(u_{xx} + u_{yy}). \tag{8}$$

It is interesting to mention that as follows from (6), the first two conditions in (5) require vanishing of the strain tensor components $u_{xz}$ and $u_{yz}$.

Condition (5) allows omitting the terms containing $u_{xz}$ and $u_{yz}$ in (4). Also using (8) and expressing $u_{zz}$ via $u_{xx} + u_{yy}$ in (4), we find the expression for the free energy density:

$$F = \frac{1}{2}\left(\lambda_{xxxx} - \frac{\lambda_{xxzz}^2}{\lambda_{zzzz}}\right)(u_{xx} + u_{yy})^2. \tag{9}$$

In addition, we impose the «incompressibility» condition, i.e., the constancy of the bulk density of the membrane:

$$u_{xx} + u_{yy} + u_{zz} = 0. \tag{10}$$

Condition (10) is satisfied simultaneously with (8) if $\lambda_{zzzz} = \lambda_{xxzz}$.

Finally, the free energy density is written as

$$F = \frac{1}{2}K_1(u_{xx} + u_{yy})^2, \tag{11}$$

where $K_1$ denotes a superposition of anisotropic elastic moduli:

$$K_1 = (\lambda_{xxxx} - \lambda_{zzzz}).$$

In the linear approximation for the strain tensor, we have

$$u_{ik} = \frac{1}{2}\left(\frac{\partial u_i}{\partial x_k} + \frac{\partial u_k}{\partial x_i}\right), \tag{12}$$

where $u_i$ is the $i$th component of the distortion field.

To introduce the essentials of our model in a simple way, we limit the following discussion to the case of a small bending amplitude, i.e., we impose condition

$$|u_z| \ll h,$$

where $u_z(\mathbf{r})$ is the $z$-component of displacement describing the deformed membrane. Also, we neglect the $z$-dependence of the component $u_z(\mathbf{r})$ in the thin plate approximation [13], thus defining the «shape» function $\xi(x, y) \approx u_z(\mathbf{r})$ independent of the depth $z$. Substituting $\xi(x, y)$ in definition (12) and then in relations (6) and conditions (5), we obtain the partial differential equations

$$\begin{aligned} \frac{\partial u_x}{\partial z} &= -\frac{\partial \xi}{\partial x}, \\ \frac{\partial u_y}{\partial z} &= -\frac{\partial \xi}{\partial y}. \end{aligned} \tag{13}$$

In integrating Eqs. (13), we introduce two functions: the (inhomogeneous) lateral stretching of the membrane $\mathbf{a}(x, y)$ and the in-plane slide $\pm\mathbf{f}(x, y)$ of the lower ($z < 0$) and upper ($z > 0$) monolayers at the mid-plane $z = 0$ of the membrane. Thus, the in-plane distortions $u_x$ and $u_y$ of each monolayer have the form

$$\begin{aligned} u_x &= -z\frac{\partial \xi(x, y)}{\partial x} + \\ &\quad + (\Theta(z) - \Theta(-z))\, f_x(x, y) + a_x(x, y), \\ u_y &= -z\frac{\partial \xi(x, y)}{\partial y} + \\ &\quad + (\Theta(z) - \Theta(-z))\, f_y(x, y) + a_y(x, y), \end{aligned} \tag{14}$$

where the step function is defined as

$$\Theta(z > 0) \equiv 1, \quad \Theta(z < 0) \equiv 0,$$

and the choice of the sign of $\Theta$ and of its argument is made for the later convenience. The step functions in (14) model splitting of the membrane into two separate monolayers and describe a discontinuity of in-plane distortions across the interface between the monolayers.

Here it is worth emphasizing the limitations of the validity of relations (14). Expressions (14) are clearly distinct from the usual expressions for thin plates [13]. In the latter case, the displacements $u_x$ and $u_y$ are set to zero at $z = 0$, implying the presence of a neutral

(not stretched) surface at the mid-plane of the plate in the small bending approximation $\xi \ll h$ [13]. It is shown in Appendix A (see Eq. (A.11)) that the second term in (14) is of the same order as the first one,

$$f_{x,y} \sim h\xi/R,$$

where $R$ is the effective radius of the membrane. The small bending approximation is justified when the term quadratic in $\xi$ is negligibly small compared to linear terms in the expressions for in-plane distortions $u_x$ and $u_y$,

$$O(\xi^2/R) \ll h\xi/R.$$

This condition is fulfilled as long as $\xi \ll h$. On the other hand, for a strongly bent thin plate, the $\xi^2$-term dominates over the $\xi$-term, and therefore higher-order terms should be added to the right-hand side of Eqs. (14).

We now discuss the physical meaning of expressions (14). The membrane stretching $\mathbf{a}(x,y)$ defines position-dependent shift of the neutral surface (along the $z$ coordinate), while the slide function $\mathbf{f}(x,y)$ multiplied by step functions leads to the splitting of this neutral surface into two surfaces belonging to the upper and lower monolayers. These surfaces are determined from the conditions

$$u_x(x,y,z) \equiv 0, \quad u_y(x,y,z) \equiv 0.$$

The function $\mathbf{f}(x,y)$ provides an additional degree of freedom in comparison with a bilayer without slide (or a single monolayer). Under the condition of zero total lateral stretching (i.e., pure bending deformation, $\mathbf{a} \equiv 0$) the presence of the function $\mathbf{f}$ means that the neutral surface splits into two such surfaces located in each monolayer symmetrically with respect to the mid-plane $z = 0$. The total amplitude of the common interlayer slide at each point $(x,y)$ of the mid-plane is then given by $2\mathbf{f}(x,y)$, which signifies discontinuity of in-plane distortions $u_x$ and $u_y$ across the mid-plane $z = 0$. In the opposite case where $\mathbf{f} \equiv 0$, the monolayers are coupled together (no interlayer slide) and the distortion field is the sum of bending and stretching (for small deformations), the latter being continuous across the mid-plane $z = 0$. In general, distortion field (14) includes bending, stretching, and mutual interlayer slide.

Substituting (14) in (12), we proceed to determine the strain tensor components for each monolayer ($z > 0$, $z < 0$):

$$\begin{aligned} u_{xx} &= -z\frac{\partial^2\xi(x,y)}{\partial x^2} + (\Theta(z) - \Theta(-z)) \times \\ &\quad \times \frac{\partial f_x(x,y)}{\partial x} + \frac{\partial a_x(x,y)}{\partial x}, \\ u_{yy} &= -z\frac{\partial^2\xi(x,y)}{\partial y^2} + (\Theta(z) - \Theta(-z)) \times \\ &\quad \times \frac{\partial f_y(x,y)}{\partial y} + \frac{\partial a_y(x,y)}{\partial y}, \end{aligned} \tag{15}$$

and $u_{zz}$ can be expressed via $u_{xx}$ and $u_{yy}$ using (8).

The above expressions allow for a free (static) mutual slide of the monolayers. The jump of the lateral strain across the interface between the monolayers does not cost elastic energy. Hence, this jump does not introduce any additional spatial scale smaller than $h$ into the problem.

The free energy functional of the whole membrane $F_v$ is obtained by integrating the free energy density $F$ over the membrane volume stepwise: first over the thickness coordinate ($-h < z < h$) and then over the membrane plane $\{x,y\}$. Using expressions (11) and (15), we finally find

$$\begin{aligned} F_v &= \frac{K_1}{2}\int (u_{xx} + u_{yy})^2 dV = \\ &= \frac{K_1}{2}\left\{\frac{2h^3}{3}\iint \left(\tilde\nabla^2\xi\right)^2 dx\,dy - \right. \\ &\quad - 2h^2\iint \left(\tilde\nabla^2\xi\right)\left(\tilde\nabla\cdot\mathbf{f}\right) dx\,dy + \\ &\quad \left. + 2h\iint \left(\left(\tilde\nabla\cdot\mathbf{a}\right)^2 + \left(\tilde\nabla\cdot\mathbf{f}\right)^2\right) dx\,dy\right\}, \end{aligned} \tag{16}$$

where the tilde refers to two-dimensional differentiation:

$$\tilde\nabla = \left\{\frac{\partial}{\partial x}, \frac{\partial}{\partial y}\right\}.$$

Equation (16) is actually quite remarkable. The mean curvature of the interlayer surface $H$ is expressed as

$$\tilde\nabla^2\xi = \frac{\partial^2\xi}{\partial x^2} + \frac{\partial^2\xi}{\partial y^2} \approx 2H. \tag{17}$$

Therefore, the first term in the right-hand side gives the effective bending energy, i.e., the extrinsic curvature-bending energy functional $F_c$ of the «standard» form [5, 13],

$$F_c = \frac{K_b}{2}\int (2H - c_0)^2 dS, \tag{18}$$

with zero spontaneous curvature $c_0$. Here, $K_b$ is the bending rigidity (modulus). Comparing (16) and (18), we find

$$2h^3K_1/3 = K_b.$$

The last term in (16) accounts for the elastic energy of area dilation with the area compression coefficient defined as

$$K_A = 2hK_1.$$

In general, the local relative area dilation $\Delta S/S$ equals $u_{xx} + u_{yy}$ [13]. According to Eq. (15), the relative area dilation is given by $\tilde{\nabla} \cdot \mathbf{a}$, while the difference of relative area dilations between the monolayers is given by $2(\tilde{\nabla} \cdot \mathbf{f})$. Hence, the $(\tilde{\nabla} \cdot \mathbf{a})^2$ term in (16) arises due to continuous (across the monolayers interface $z = 0$) lateral stretching of the membrane, which leads to a change in the average lipid density. The $(\tilde{\nabla} \cdot \mathbf{f})^2$ term represents the energy of local area difference of the monolayers (area-difference elasticity [2]), which is equivalent to the difference of lipid densities in monolayers (density-difference model [9]). In principle, this energy is not related to the presence of neutral surfaces within the monolayers (at large membrane stretching/compression, there are no neutral surfaces that would obey $u_x \equiv u_y \equiv 0$, see expression (14)). As is apparent from Eq. (16), the relation between bending and area compression coefficients (see [2])

$$K_b/K_A \sim h^2$$

occurs naturally in our derivation.

Next, the second term in the right-hand side of Eq. (16) expresses the coupling between bending deformation and interlayer slide producing a local area dilation difference between monolayers. We note that in the lowest-order approximation, bending is decoupled from (continuous) area dilation caused by lateral stretching. Due to the hydrophobic effect, the monolayers, while sliding, are forced to stick together and to follow the same shape defined by $\xi(x, y)$ on the monolayer interface. Mutual interlayer slide along the interface leads to relaxation of stretching/compression of the monolayers caused by bending deformation, and thus permits the free energy decrease.

Finally, our free energy functional is invariant with respect to transversal slide of monolayers such that $\mathrm{div}\,\mathbf{f} = 0$. Hence, the energy does not change under mutual rotation of the monolayers (as a whole) or a position-independent shift of one of the monolayers with respect to the other.

We consider pure bending deformations of the membrane with no overall stretching. Therefore, we require the lateral strain integrated over the thickness to be zero at each point of the membrane. This imposes a restriction on the form of $u_x$ and $u_y$: the function $\mathbf{a}(x, y)$ must be equal to zero at every point of the bilayer. Hence, this function is omitted everywhere below. Then the strain tensor components can be written as

$$\begin{aligned} u_{xx} &= -z\frac{\partial^2 \xi}{\partial x^2} + (\Theta(z) - \Theta(-z))\,\frac{\partial f_x}{\partial x}, \\ u_{yy} &= -z\frac{\partial^2 \xi}{\partial y^2} + (\Theta(z) - \Theta(-z))\,\frac{\partial f_y}{\partial y}, \end{aligned} \tag{19}$$

and $u_{zz}$ can again be expressed via $u_{xx}$ and $u_{yy}$ using (8).

The free energy functional of the membrane acquires the form

$$\begin{aligned} F_v = \frac{K_1}{2}\int (u_{xx} + u_{yy})^2 dV = \\ = \frac{K_1}{2}\left\{\frac{2h^3}{3}\iint \left(\tilde{\nabla}^2\xi\right)^2 dx\,dy - 2h^2 \times \right. \\ \times \iint \left(\tilde{\nabla}^2\xi\right)\left(\tilde{\nabla}\cdot\bar{\mathbf{f}}\right) dx\,dy + \\ \left. + 2h\iint \left(\tilde{\nabla}\cdot\bar{\mathbf{f}}\right)^2 dx\,dy\right\}. \end{aligned} \tag{20}$$

To study the properties of functional (20) in detail, a simple problem with cylindrically symmetric deformation is discussed in Appendix A. The equilibrium of the membrane is defined by the Euler–Lagrange equations, which are obtained by equating to zero the first variational derivatives of the elastic energy functional $F(\xi, f)$ with respect to the functions $\xi(r)$ and $f(r)$.

## 3. CONFINING POTENTIAL FOR A BILAYER WITH SLIDE

Direct influence of the confined geometry on the membrane behavior manifests itself in a reduction of the manifold of accessible membrane conformations. Entropic interactions of the membrane with confining walls (see Fig. 1) can be modeled [12] by introduction of an extra potential energy $W$ dependent on the bending amplitude,

$$W = \frac{\alpha}{2}\xi^2.$$

The free energy functional (20) appended with the confining potential $W$ acquires the form

$$\begin{aligned} F_v = \frac{K_1}{2}\left\{\frac{2h^3}{3}\iint \left(\tilde{\nabla}^2\xi\right)^2 dx\,dy - \right. \\ - 2h^2\iint \left(\tilde{\nabla}^2\xi\right)\left(\tilde{\nabla}\cdot\mathbf{f}\right) dx\,dy + \\ \left. + 2h\iint \left(\tilde{\nabla}\cdot\mathbf{f}\right)^2 dx\,dy\right\} + \frac{\alpha}{2}\iint \xi^2 dx\,dy. \end{aligned} \tag{21}$$

The curvature of the confining potential at its minimum,

$$\alpha = \left.\frac{d^2W}{d\xi^2}\right|_{\xi=0},$$

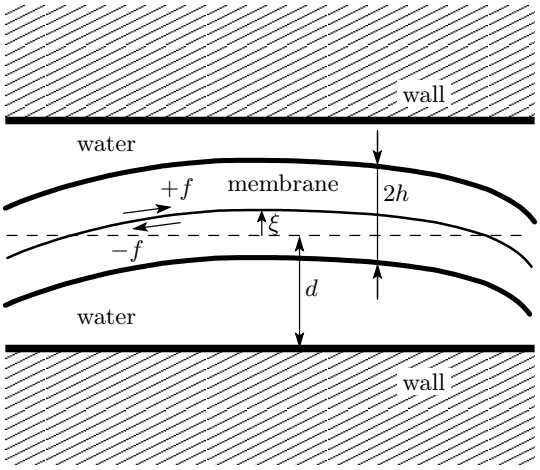


**Fig. 1.** Membrane in the confined geometry. A bilayer membrane (each monolayer of thickness $h$) is placed in water solution between parallel walls separated by distance $2d$. The bending amplitude $\xi = u_z$ is defined at the mid-plane and is independent of the depth in the membrane. The interlayer slide function $\mathbf{f}$ parameterizes position-dependent mutual slide of the monolayers at their interface

is calculated below using a self-consistent procedure.

In the Fourier space $\mathbf{q} = \{q_x, q_y\}$, free energy functional (21) is written as

$$F_v = \int_0^\infty \int_0^\infty \left( K_1 \frac{2h^3}{3} q^4 + \alpha \right) |\xi_q|^2 \frac{dq_x dq_y}{(2\pi)^2} - \\ - \int_0^\infty \int_0^\infty K_1 h^2 i q^2 (\xi_q \mathbf{q}\cdot\mathbf{f}_q^* - \xi_q^* \mathbf{q}\cdot\mathbf{f}_q) \frac{dq_x dq_y}{(2\pi)^2} + \\ + \int_0^\infty \int_0^\infty 2K_1 h |\mathbf{q}\cdot\mathbf{f}_q|^2 \frac{dq_x dq_y}{(2\pi)^2}, \quad (22)$$

where

$$q^2 = q_x^2 + q_y^2.$$

We diagonalize the quadratic form in (22) with respect to $\xi_q$ and $\mathbf{q}\cdot\mathbf{f}_q$ by the linear transformation

$$\begin{aligned} \operatorname{Re}\tilde{\xi}_q &= \operatorname{Re}\xi_q - \frac{3}{2h}\frac{q^2}{\tilde{q}^4}\operatorname{Im}(\mathbf{q}\cdot\mathbf{f}_q), \\ \operatorname{Im}\tilde{\xi}_q &= \operatorname{Im}\xi_q + \frac{3}{2h}\frac{q^2}{\tilde{q}^4}\operatorname{Re}(\mathbf{q}\cdot\mathbf{f}_q), \end{aligned} \quad (23)$$

where

$$\tilde{q}^4 = q^4 + \frac{\alpha}{K_b}, \quad K_b = \frac{2h^3}{3}K_1.$$

In terms of the variables $\tilde{\xi}_q$ and $\mathbf{f}_q$, energy functional (22) becomes

$$F_v = \int_0^\infty \int_0^\infty \frac{K_1}{2} \left\{ \frac{4h^3}{3}\tilde{q}^4 |\tilde{\xi}_q|^2 + \right. \\ \left. + h\left(4 - 3\left(\frac{q}{\tilde{q}}\right)^4\right) |\mathbf{q}\cdot\mathbf{f}_q|^2 \right\} \frac{dq_x dq_y}{(2\pi)^2}. \quad (24)$$

Using relations (23) and functional (24), we calculate the thermodynamic average

$$\langle |\xi_q|^2 \rangle = \frac{k_B T}{\frac{2h^3}{3}K_1 q^4 + \alpha} + \\ + \frac{3q^4 k_B T}{\left(\frac{2h^3}{3}K_1 q^4 + \alpha\right)\left(q^4 + \frac{6\alpha}{K_1 h^3}\right)}, \quad (25)$$

where $k_B$ is the Boltzmann constant and $T$ is the temperature.

In the absence of interlayer slide, only the first term remains in Eq. (25), as obtained in [12, 15]. The second term in (25) signifies enhancement of the bending fluctuations caused by interlayer slide. The latter leads to relaxation of the lateral stresses (see Appendix A and Fig. 3 below) and thus to a decrease of the free energy of the bent membrane.

The mean-square fluctuations of the bending amplitude are found as

$$\langle \xi^2(\bar{r}) \rangle = \int_0^\infty \langle |\xi_q|^2 \rangle q \frac{dq}{2\pi} = \sqrt{\frac{3}{32}} \frac{k_B T}{\sqrt{\alpha K_1 h^3}}. \quad (26)$$

In the confined geometry, the average bending amplitude is restricted to the finite two-dimensional space between the walls (neglecting the volume occupied by the membrane itself, i.e., $h \ll d$), thus providing the self-consistency condition for determination of the effective rigidity $\alpha$,

$$\langle \xi^2 \rangle = \mu d^2, \quad (27)$$

where $\mu \le 1$.

Substituting (26) in (27), we obtain a self-consistent solution for $\alpha$:

$$\alpha = \frac{(k_B T)^2}{16\mu^2 d^4 K_b}. \quad (28)$$

We here also evaluate the curvature $\alpha_0$ of the confining potential for a unit bilayer (without interlayer slide). In this case, the second term in the right-hand side of (25) is zero, and hence

$$\alpha_0 = \frac{(k_B T)^2}{64\mu^2 d^4 K_b}. \quad (29)$$

Thus, interlayer slide results in considerable enhancement ($\alpha/\alpha_0 = 4$) of the curvature of the confining potential.

## 4. BILAYER DYNAMICS: VISCOUS MODES

To study the dynamical properties of the introduced model of a bilayer membrane with interlayer slide, we here determine the equations of motion and find the eigenmodes of the membrane surrounded by water solution. We are interested in the behavior of the membrane confined between parallel walls (see Fig. 1).

Let a flat membrane lie in the $xy$ plane with the normal pointed along the $z$ axis. We treat each monolayer constituting the membrane as a (unit) two-dimensional condensed structure. We require the equilibrium between viscous stresses exerted on the membrane surface by water solution and the membrane restoring force. We neglect inertial effects and introduce three sources of viscous dissipation: water and membrane viscosities and interlayer drag. The force balance equations are expressed as

$$-\frac{\delta F_s}{\delta \xi} + \Pi_{zz}(z=+0) - \Pi_{zz}(z=-0) = 0, \qquad (30)$$

$$\frac{\delta F_s}{\delta f_x} - 2\eta_m h \frac{\partial}{\partial t}\left(\tilde{\nabla}^2 f_x\right) + 2b_s \frac{\partial f_x}{\partial t} - \\ - \Pi_{xz}(z=+0) - \Pi_{xz}(z=-0) = 0, \qquad (31)$$

$$\Pi_{xz}(z=+0) - \Pi_{xz}(z=-0) = 0. \qquad (32)$$

Here, the fluid stress tensor is defined as

$$\Pi_{ik} = -p\delta_{ik} + \eta_w\left(\frac{\partial v_i}{\partial x_k} + \frac{\partial v_k}{\partial x_i}\right),$$

where $p$ denotes the hydrostatic pressure, $\mathbf{v}$ is the velocity, and $\eta_w$ is the viscosity of water solution. The fluid stress tensor is evaluated at the upper ($z = +0$) and lower ($z = -0$) membrane surfaces and carries the sign of the normal. The first term in the left-hand side of Eq. (30) is the elastic restoring membrane force, which is balanced by viscous stress of the fluid normal to the membrane surface. Equation (31) represents force balance in the lateral direction and contains the following contributions [3, 9]: a) tangential traction on the interlayer surface due to differential flow of monolayers; b) coherent surface flow of the monolayers as unit surfaces (with the dynamic viscosity $\eta_m$); c) viscous drag between monolayers (characterized by the coefficient $b_s$) that arises at a finite velocity of their mutual slide; d) traction of the surrounding fluid. Equation (32) accounts for the absence of total stretching forces exerted by water on the membrane because we here discuss only pure bending deformations of the membrane, i.e., when the total area dilation is zero.

Navier–Stokes equations for water solutions surrounding the membrane should be added to balance Eqs. (30)–(32). In the small-velocity limit, treating fluid as incompressible and neglecting inertia, we write the «creeping flow» equations as

$$\begin{aligned} \nabla p &= \eta_w \Delta v, \\ \nabla \cdot \mathbf{v} &= 0. \end{aligned} \qquad (33)$$

The non-slip boundary conditions at the membrane–water interface provide the continuity of normal and tangential velocities of the fluid and the membrane:

$$\frac{\partial \xi}{\partial t} = v_z(\pm 0), \qquad (34)$$

$$\begin{aligned} \frac{\partial f_i}{\partial t} &= v_i(z=+0), \\ -\frac{\partial f_i}{\partial t} &= v_i(z=-0), \quad i = x, y. \end{aligned} \qquad (35)$$

Confinement between parallel walls at the distance $2d$ implies vanishing of water velocity (normal and tangential components) at the walls surfaces:

$$v_j(z = \pm d) = 0, \quad j = x, y, z. \qquad (36)$$

To find the dispersion relation, we make the Fourier transform of free energy functional (21) and of the force balance and creeping flow equations. For this, we expand the vibration in plane waves propagating along the $x$ direction. The free energy density $F_s(q, \omega)$ then takes the form

$$F_s(q,\omega) = \frac{K_1}{2}\left\{\frac{4h^3}{3}q^4|\xi_q|^2 - \right. \\ \left. - 2h^2(\xi_q f_q^* - \xi_q^* f_q)q^3 i + 4h|f_q|^2 q^2\right\} + \alpha|\xi_q|^2 \qquad (37)$$

and

$$F_v = \frac{L_y}{(2\pi)^2}\int\limits_{-\infty}^{+\infty}\int\limits_{0}^{+\infty} F_s(q,\omega)\, dq\, d\omega, \qquad (38)$$

where $L_y$ is the system dimension along the $y$ axis, and we have omitted the index $\omega$ in the subscripts of Fourier components.

The restoring membrane forces are given by functional derivatives of the free energy,

$$\frac{\delta F_s}{\delta \xi_q^*} = \left(K_1\frac{2h^3}{3}q^4 + \alpha\right)\xi_q + K_1 h^2 f_q q^3 i, \qquad (39)$$

$$\frac{\delta F_s}{\delta f_q^*} = -K_1 h^2 \xi_q q^3 i + 2K_1 h q^2 f_q. \qquad (40)$$

Fourier transforms of creeping flow equations (33) for the components of water velocity and pressure

$$v_x = w_x(z)\exp(iqx - i\omega t), \quad v_z = w_z(z)\exp(iqx - i\omega t),$$

$$p = p_q(z)\exp(iqx - i\omega t)$$

are written as

$$iqw_x + \frac{\partial w_z}{\partial z} = 0,$$

$$iqp_q = \eta_w\left(-q^2 w_x + \frac{\partial^2 w_x}{\partial z^2}\right),$$

$$\frac{\partial p_q}{\partial z} = \eta_w\left(-q^2 w_z + \frac{\partial^2 w_z}{\partial z^2}\right). \qquad (41)$$

We find the following solutions of differential equations (41) with the normal velocity continuous at $z = 0$, also obeying the condition of zero lateral stretching force acting on the membrane (equation (32)) and the condition

$$v_x(z = +0) = -v_x(z = -0)$$

resulting from Eq. (35):

$$p_q = \begin{cases} 2\eta_w(C_1 e^{qz} + C_2 e^{-qz}), & z > 0, \\ 2\eta_w(-C_1 e^{-qz} - C_2 e^{qz}), & z < 0, \end{cases} \qquad (42)$$

$$w_z = \begin{cases} [C_1 z + C_3]e^{qz} + [C_2 z + C_4]e^{-qz}, & z > 0, \\ [-C_1 z + C_3]e^{-qz} + [-C_2 z + C_4]e^{qz}, & z < 0, \end{cases} \qquad (43)$$

$$w_x = \begin{cases} \left[C_1 z + C_3 + \dfrac{C_1}{q}\right] ie^{qz} + \left[-C_2 z - C_4 + \dfrac{C_2}{q}\right] ie^{-qz}, & z > 0, \\ \left[-C_2 z + C_4 - \dfrac{C_2}{q}\right] ie^{qz} + \left[C_1 z - C_3 - \dfrac{C_1}{q}\right] ie^{-qz}, & z < 0. \end{cases} \qquad (44)$$

This solution maintains the symmetry relations compatible with the confined geometry:

$$w_x\left(z, x + \frac{\pi}{q}\right) = w_x(-z, x),$$

$$w_z\left(z, x + \frac{\pi}{q}\right) = -w_z(-z, x). \qquad (45)$$

Physical meaning of Eq. (45), according to the definitions given before (41), is that the $x/z$-component of water velocity around a vibrating membrane behaves symmetrically/antisymmetrically under simultaneous translation by the half-period ($x \to x + \pi/q$) along the wave propagation direction $x$ and mirror reflection in the mid-plane between the confining walls ($z \to -z$).

We next eliminate the unknown coefficients $C_2$ and $C_4$ using stick boundary conditions at the walls, Eq. (36). We then substitute the solutions in form (42)–(44) into Fourier-transformed force balance equations (30) and (31) (exploiting (39) and (40)) and into non-slip conditions (34) and (35) at the water–membrane interface. Thus, we finally obtain the algebraic system of four linear homogeneous equations for the unknowns $C_1$, $C_3$, $\xi_q$, and $f_q$:

$$\xi_q\left[-\frac{2h^3}{3}K_1 q^4 - \alpha\right] + f_q[-K_1 h^2 i q^3] + C_1[-4\eta_w 2q^2 d^2 e^{2qd}] + C_3\left[4\eta_w q(1 + e^{2qd} - 2qde^{2qd})\right] = 0, \qquad (46)$$

$$\xi_q(-h^2 K_1 q^3 i - 4\eta_w q\omega) + f_q(2K_1 h q^2 - 2\eta_m h q^2 i\omega - 2b_s i\omega) + C_1[-4\eta_w i(1 + e^{2qd} + 2qde^{2qd})] + C_3[-4\eta_w i 2q e^{2qd}] = 0, \qquad (47)$$

$$i\omega\xi_q + 2qd^2 e^{2qd} C_1 + C_3(1 + 2qde^{2qd} - e^{2qd}) = 0, \qquad (48)$$

$$\omega f_q + \frac{C_1}{q}(1 - e^{2qd} - 2qde^{2qd} - 2q^2 d^2 e^{2qd}) + C_3(1 - 2qde^{2qd} - e^{2qd}) = 0. \qquad (49)$$

The dispersion relation $\omega(q)$ is found by equating the determinant of system (46)–(49) to zero. The latter gives a quadratic equation for $\omega(q)$ that results in two branches $\omega_1(q)$ and $\omega_2(q)$, see Fig. 2. Two viscous modes — the hydrodynamically damped bending mode and the intermonolayer slipping mode — mix, and the power law $\omega(q)$ changes with the wavelength of fluctuations. For pure bending deformation of the membrane, there exist up to four hydrodynamic regimes (depending on the parameters of the system), separated by three crossover wave vectors.

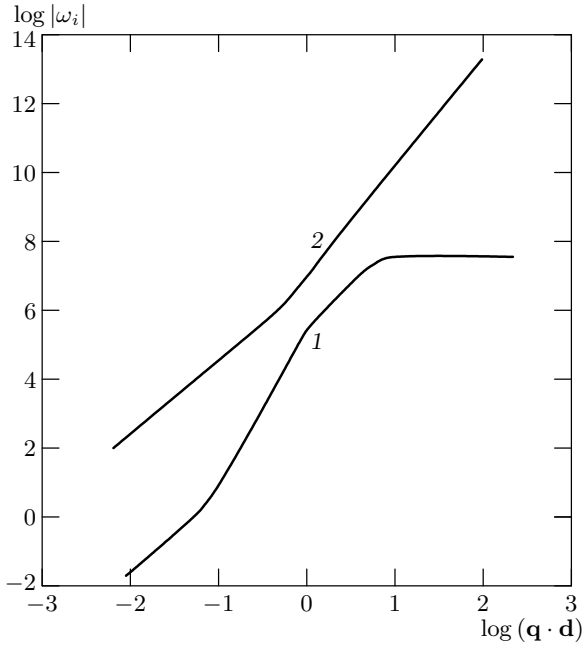


**Fig. 2.** Viscous modes of a bilayer membrane in water solution confined between parallel walls in the case of pure bending deformations. Damping rates $|\omega_i|$ [1/s] are plotted as functions of the dimensionless parameter $(\mathbf{q}\cdot\mathbf{d})$, where $\mathbf{q}$ is the wave vector and $2d$ is the distance between the walls. Two branches *1* and *2* originate from bending and interlayer slide. The following values of parameters are used: $d = 10^{-6}$ cm, $h = 2\cdot 10^{-7}$ cm, $\eta_w = 10^{-2}$ dyn · s/cm$^2$, $\eta_m = 1$ dyn · s/cm$^2$, $b_s = 10^7$ dyn · s/cm$^3$, $K_1 = 2\cdot 10^8$ erg/cm$^3$

We use the result in (28) to estimate the upper limit $q_0$ of the smallest $q$ interval where the eigenmodes are modified by the confining potential, i.e., where the induced rigidity term ($\sim \alpha$) dominates over the bending term ($\sim K_b q^4$) in (22) (and in the first bracket in Eq. (46)):

$$q \ll q_0 \equiv \left(\frac{\alpha}{K_b}\right)^{1/4} = \left(\frac{k_B T}{K_b}\right)^{1/2} \frac{1}{2d} \left(\frac{1}{\mu}\right)^{1/2}. \quad (50)$$

For a typical value of bending rigidity at room temperature [2]

$$K_b \approx 25 k_B T,$$

we obtain

$$q_0 \sim \frac{0.1}{d}.$$

The second crossover wave vector $1/d$ bounds the long-wavelength regime where confinement of the surrounding water between the walls affects membrane dynamics. For $q \gg 1/d$, the membrane behaves as in the bulk water solution. We assume that the distance between confining walls is much greater than the monolayer thickness ($2d/h \sim 10$). The crossover wave vector for the bulk fluid $q_1$ (see Appendix B) for the chosen parameters $h = 2\cdot 10^{-7}$ cm, $\eta_w = 10^{-2}$ dyn · s/cm$^2$, and $b_s = 10^7$ dyn · s/cm$^3$ acquires the value

$$q_1 = \frac{\eta_w}{b_s h^2} \sim 10^5 \text{ cm}^{-1}$$

and therefore obeys the condition $q_1 \ll 1/d$. Therefore, it does not influence dynamic behavior of the membrane in the confined geometry. In the interval of even shorter wavelengths, there is one more crossover wave vector

$$q_2 = \sqrt{\frac{b_s}{\eta_m h}} \approx \frac{10^7}{\sqrt{2}} \text{ cm}^{-1}$$

($\eta_m = 1$ dyn · s/cm$^2$), which obeys the condition $1/d \ll q_2$. Hence, we investigate four intervals of wave vector values:

$$q \ll q_0,$$

$$q_0 \ll q \ll 1/d,$$

$$1/d \ll q \ll q_2,$$

$$q_2 \ll q.$$

For long wavelengths, $q \ll 1/d$, confinement between the walls modifies the bending mode with respect to the membrane in the bulk solution (see Appendix B),

$$\omega_1^B = -iq^3 \frac{K_1 h^3}{24\eta_w} \approx -iq^3 \frac{K_b}{\eta_w}, \quad (51)$$

and results in either $q^2$- or $q^6$-dependences of $\omega_1$ instead of the $q^3$-dependence of the «bulk» mode. For $q \ll q_0$, the bending mode becomes (to be compared with [16])

$$\omega_1 = -iq^2 \frac{\alpha d^3}{24\eta_w}. \quad (52)$$

The mode $\omega_1(q)$ is driven by the entropic potential, characterized by curvature $\alpha$, and is damped by viscous losses in the surrounding fluid. It is interesting to mention that for a bilayer with interlayer slide, $\alpha$ is four times greater that for a unit bilayer (see Eqs. (28) and (29)). Thus, interlayer slide leads to faster dynamics of the membrane.

For $q_0 \ll q \ll 1/d$, the hydrodynamically damped bending mode is given by

$$\omega_1 = -iq^6 \frac{K_1 h^3 d^3}{144\eta_w} \approx -iq^6 \frac{K_b d^3}{\eta_w}. \quad (53)$$

In this wave vector interval, the finite thickness $d$ of water layers effectively enhances water viscosity from

$\eta_w$ to $\eta_w/(dq)^3 \gg \eta_w$. Result (47) coincides (modulo a numeric coefficient) with the damped vibration mode of erythrocyte walls consisting of two membranes with liquid between them [6].

On the other hand, intermonolayer slipping mode $\omega_2(q)$, damped by viscous drag at the monolayer mutual interface, remains unchanged by confinement (see Appendix B):

$$\omega_2 = -iq^2 \frac{K_1 h}{b_s} \approx -iq^2 \frac{K_A}{b_s}\,. \tag{54}$$

For a membrane in the bulk solution, mixing of the bending and slipping modes occurs at $q \approx q_1$, see Appendix B. The relative order of the parameters $q_1$, $1/d$, and $q_2$ by increasing value depends on the choice of characteristic parameters of the system. With our choice, $q_1 \ll 1/d$ and the mixing of the modes is delayed up to $q \approx 1/d$, see Fig. 2. We speculate that this happens because confinement hinders bending fluctuations and therefore the bending mode remains slower than the slipping mode up to $q \approx 1/d$.

In the short-wavelength limit $q \gg 1/d$, we recover, as expected, the result for a membrane in the bulk water. Confinement is not revealed in this case because membrane-induced vibrations of water decay exponentially before reaching the walls. Namely, for $q \gg 1/d$, the branch $\omega_2(q)$ now corresponds to the bending mode damped by viscous losses in the surrounding fluid:

$$\omega_2^B = -iq^3 \frac{K_1 h^3}{6\eta_w} \approx -iq^3 \frac{K_b}{\eta_w}\,. \tag{55}$$

The renormalized bending rigidity ($\sim K_1 h^3$) arises for high-frequency fluctuations (to be compared with the numeric coefficients in (51) and in (55)) because the bending mode is faster than the interlayer slipping mode [9, 10]; interlayer slide leading to relaxation of lateral stresses in monolayers is retarded. In the interval $1/d \ll q \ll q_2$, the branch $\omega_1(q)$ becomes the interlayer slipping mode with the renormalized area compression modulus

$$\omega_1^B = -iq^2 \frac{K_1 h}{4b_s} \approx -iq^2 \frac{K_A}{b_s}\,, \tag{56}$$

(the superscript «$B$» indicates that the solution coincides with the bulk water case). Finally, for $q \gg q_2$, the $\omega_1(q)$ mode is driven by the (high-frequency) effective rigidity $K_1$ and is damped by the monolayer surface viscosity $\eta_m$, which dominates over interlayer drag as the monolayers are dynamically coupled:

$$\omega_1^B = -i \frac{K_1}{4\eta_m}\,. \tag{57}$$

The viscous modes for a membrane in confined geometry obtained in this paper qualitatively agree with the results for a membrane bound to substrate [10]. We have not included the membrane tension into our free energy functional because in the considered limit of small bending deformations of the bilayer, the term proportional to the gradient of the bending amplitude is negligible [15].

The dispersion relation for a bilayer membrane in the bulk water based on our free energy functional (20) is derived in Appendix B and also agrees with earlier results obtained using the density-difference model [9].

## 5. CONCLUSIONS

A novel free energy functional of a bilayer fluid membrane derived in this paper reflects important physical properties of the membrane defining its dynamic behavior. The functional allows for two-dimensional liquid-crystalline structure of the membrane and weak adherence between the monolayers constituting it, leading to their mutual slide under (bending) deformations. Our free energy functional contains three coupled fields parameterizing the degrees of freedom related to bending of the membrane, interlayer mutual slide, and area dilation.

Using this functional, we have self-consistently calculated the curvature of the effective entropic potential acting on the membrane between two parallel confining walls. We found that the curvature at the potential minimum (located at the middle between the walls) is enhanced four times for a bilayer with interlayer slide in comparison with a unit membrane (with forbidden slide) of the same thickness. This leads to faster dynamics. This increase can be ascribed to (partial) decrease of the lateral stress in the bent membrane via interlayer slide (static softening of the membrane). The relaxation of stresses effectively lowers the energetic «cost» of membrane bending and increases the thermodynamic probability for conformations with greater bending amplitudes. This in turn amplifies entropic repulsion.

We have also calculated the dispersion relations for a membrane confined between parallel walls. Our results are in qualitative agreement with those for a membrane bound to a substrate [10]. Confinement modifies the viscous modes $\omega(q)$ at long wavelengths compared to the bulk water case. We have found four wave-vector intervals separated by three characteristic wave-vector values, $q_0 \ll 1/d \ll q_2$, defined in Sec. 4. The inverse of the half-distance $d$ between the confining walls divides

the $q$ axis into two intervals with confined ($q \ll 1/d$) and bulk ($q \gg 1/d$) behavior, respectively. The wave vector $q_0$ delimits the interval of $q$ values in which the entropic potential modifies the spectrum of bending modes (see also [16]). In the interval $q_0 \ll q \ll 1/d$, we found the dependence of bending mode

$$\omega(q) \propto q^6,$$

similar to peristaltic modes of a soap film [6]. Unlike in [10], we do not obtain the dependence

$$\omega(q) \propto q^4,$$

because the overall membrane tension is not included into our free energy functional. Because we consider the limit of small bending deformations of a flat bilayer, the term proportional to the gradient of the bending amplitude vanishes [15]. In the interval $q \gg 1/d$, confinement is not important because membrane-induced vibrations of water decay exponentially before reaching the walls. At $q > q_2$, as in the bulk case, the monolayer surface viscosity $\eta_m$ dominates over the interlayer drag and the monolayers become dynamically strongly coupled.

Finally, we mention some limitations and possible improvements of our approach. Our functional respects reflectional symmetry of a flat bilayer and therefore implies that spontaneous curvature is zero. We assumed a thin-plate approximation for each monolayer with constant elastic moduli. In other words, we developed a phenomenological effective medium model. Hence, only fluctuations with wavelengths larger than the intermolecular distance in a lipid monolayer are considered. We have exploited smallness of the bending-to-thickness ratio using the linear approximation for the stress tensor. In the small-bending approximation, area dilation is decoupled from bending. In this paper, we discussed only pure bending deformations, but the area dilation dynamics can also be studied using our functional. We found only damped eigenmodes of the membrane in confined water solution. The propagating modes will be considered elsewhere.

The authors are grateful to Prof. R. Bruinsma for the formulation of the problem and to Prof. Yu. A. Chizmadzhev and his coworkers for useful comments. The work of S. B. is supported by the Nonprofit Foundation «Dynasty» and the PhD student grant A03-2.9-283 of the Russian Ministry of Education.

## APPENDIX A

### Analytic solutions in the axially symmetric case

We can obtain analytic results describing the equilibrium shape of and mutual monolayer slide in the bilayer lipid membrane under constant external pressure in the cylindrically symmetric case. We consider a flat (unperturbed) circular membrane of the radius $R$ in the plane $xy$. We search for an equilibrium solution independent of the polar angle $\phi$,

$$\xi = \xi(r), \tag{A.1}$$

where $r$ is the radial coordinate in the reference system with the origin at the center of the unperturbed membrane mid-plane and with the $z$ axis directed along the membrane normal. Hence, the slide functions take the form

$$f_x(x,y) = f(r)\cos\phi, \quad f_y(x,y) = f(r)\sin\phi, \tag{A.2}$$

which then leads to the following expression for the radial component of the distortion field:

$$u_r(r,z) = -z\frac{\partial\xi(r)}{\partial r} + (\Theta(z) - \Theta(-z))\, f(r). \tag{A.3}$$

Because the deformation is purely radial, the angular component of the distortion is zero:

$$u_\phi = 0.$$

The symmetry of distortion fields (A.1) and (A.2) allows expressing the free energy density (11) in the cylindrical coordinates as

$$F = \frac{K_1}{2}(u_{rr} + u_{\phi\phi})^2, \tag{A.4}$$

where

$$u_{rr} = \frac{\partial u_r}{\partial r}, \quad u_{\phi\phi} = \frac{u_r}{r} + \frac{1}{r}\frac{\partial u_\phi}{\partial \phi} = \frac{u_r}{r}\,. \tag{A.5}$$

The equilibrium of the membrane under pressure is defined by the Euler–Lagrange equations, which are obtained by equating to zero the first variational derivatives of the elastic energy functional $F(\xi, f)$ with respect to the functions $\xi(r)$ and $f(r)$ entering $u_{rr}$ and $u_{\phi\phi}$ in accordance with (A.5) and (A.3),

$$\begin{aligned} &\frac{\delta F_{sr}}{\delta\xi(r)} - 2\pi r P = 0, \\ &\frac{\delta F_{sr}}{\delta f(r)} = 0, \end{aligned} \tag{A.6}$$

where

$$F_v = \int_0^R F_{sr} dr$$

and $P$ is the $z$-component of the external pressure difference applied to the opposite sides of the membrane.

Equations (A.6) can be decoupled by introducing the new unknown functions $p(r)$ and $g(r)$ instead of $\xi$ and $f$:

$$p = \frac{4h}{3}\frac{\partial \xi}{\partial r} - 2f, \quad g = h\frac{\partial \xi}{\partial r} - 2f. \tag{A.7}$$

In the new basic set of functions $\{p, g\}$, Eqs. (A.6) become

$$\begin{aligned} &r^3 p''' + 2r^2 p'' - rp' + p = P_1 r^3, \\ &r^2 g'' + rg' - g = 0, \end{aligned} \tag{A.8}$$

where

$$P_1 = \frac{2P}{K_1 h^2}.$$

Both equations in (A.8) belong to the Euler class of equations and can be solved analytically using the transformation of the variable,

$$r = e^x,$$

where $-\infty < x < \infty$ is the new variable.

The following boundary conditions are imposed.

1) $(p''(r)r + p'(r) - p(r)/r)\,|_{r=0} = 0$ — the bending amplitude $\xi(r)$ is arbitrary at $r = 0$;

2) $\xi(R) = 0$ — the membrane is fixed at the edge (no vertical displacement);

3) $(p'(r)r + p(r))\,|_{r=R} = 0$ — zero torque at the membrane edge;

4) $\partial\xi/\partial r|_{r=0} = 0$ — the slope at the center is zero;

5) $f(0) = 0$ — no intermonolayer slide at the center (axial symmetry);

6) $g'(r)r + g(r)|_{r=R} = 0$ — the intermonolayer slide at the edge is arbitrary.

These conditions have transparent physical meaning. Conditions 1) and 3) originate from the expression for the variational derivative $\delta F_{sr}/\delta\xi$, and condition 6) arises in the variational derivative $\delta F_{sr}/\delta f$; both derivatives include integration by parts in the segment $[0 \le r \le R]$. In particular, condition 1) is obtained by equating the prefactor in front of $\delta\xi(r = 0)$ to zero. Condition 3) is derived by equating the prefactor in front of $\partial\xi/\partial r|_{r=R}$ to zero, which in turn corresponds to zero torque $M$ at the membrane edge (hence, the membrane slope at the edge is arbitrary):

$$M = K_1 \pi h^2 \times \left(\frac{4}{3}h\left(\frac{\partial^2 \xi}{\partial r^2}r + \frac{\partial \xi}{\partial r}\right) - 2\left(\frac{\partial f}{\partial r}r + f\right)\right). \tag{A.9}$$

Condition 2) models the fixation of the membrane at the periphery. Condition 4) implies a smooth shape at the center of the curved membrane. The resulting solutions are

$$\begin{aligned} \xi(r) &= \frac{3P}{32K_1h^3}(r^4 - 4R^2r^2 + 3R^4), \\ f(r) &= \frac{3P}{16K_1h^2}(r^3 - 2R^2r). \end{aligned} \tag{A.10}$$

The bending amplitude $\xi(r) = u_z(r)$ is defined at the interface (mid-plane) of the membrane and is $z$-independent (for small bending of the membrane considered here). The function $f(r)$ characterizes the amplitude of mutual slide of the monolayers at the interface of the membrane ($z = 0$) (the total amplitude is given by $2f$). As a result of this slide, the bottom surface of the upper monolayer is compressed, and the top surface of the lower monolayer is expanded. In the present approximate approach, $f$ is constant along the thickness (along the $z$ axis) of the monolayers and depends on the position in the plane of the membrane. It is apparent from (A.10) that

$$f \sim h\xi/R.$$

Substituting (A.10) in expression (A.3) for the radial distortion $u_r$, we find

$$u_r = \frac{3P}{16K_1h^2}\left(-z\frac{2}{h} - \Theta(-z) + \Theta(z)\right) \times (r^3 - 2R^2r). \tag{A.11}$$

The radial stress component corresponding to the distortion given by (A.11) is readily found as

$$\sigma_{rr}(r, z) = \frac{3P}{4h^2}\left(-z\frac{2}{h} - \Theta(-z) + \Theta(z)\right) \times (r^2 - R^2). \tag{A.12}$$

It is important to mention here that the lateral stress component $\sigma_{rr}$ in (A.12) proves to be independent of the elastic modulus ($K_1$) in our weak bending approximation. On the other hand, the distortion and slide fields and the strain tensor components depend on the elastic modulus.

In the considered case of a small bending amplitude, there is no overall stretch of the deformed membrane (i.e., pure bending occurs) and thus at any $r$:

$$\int_{-h}^{h} \sigma_{rr}(r)\, dz \approx \int_{-h}^{h} [u_{rr}(r) + u_{\phi\phi}(r)]\, dz = 0. \tag{A.13}$$

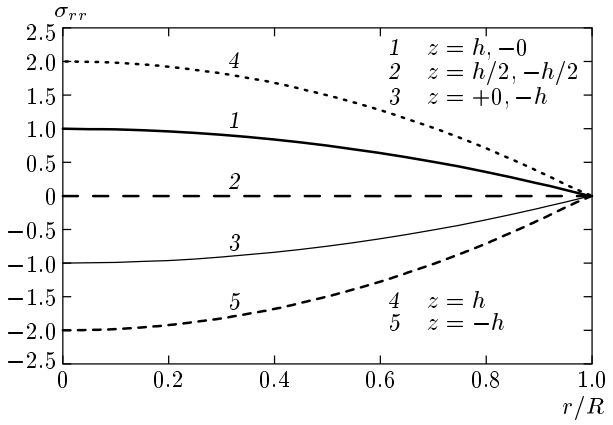


**Fig. 3.** The lateral stress $\sigma_{rr}$ normalized by $3PR^2/4h^2$ for various $z$-positions inside the membrane ($z > 0$ for the upper monolayer and $z < 0$ for the lower) is plotted as a function of the radial coordinate $r$ (in dimensionless units). The solid lines show stresses in the upper and lower monolayers (the stress profiles along the $z$ axis in both monolayers coincide due to interlayer slide, see text). The dashed line represents two neutral surfaces (at $z = \pm h/2$) in the lower und upper monolayers. The dotted lines ($z = h$, $z = -h$) characterize the stresses in the membrane of the same thickness $2h$ with forbidden slide

The $z$-dependent factor in Eq. (A.12) guarantees that Eq. (A.13) is satisfied. Condition (A.13) is kept by the equality of the factors in front of $\Theta(+z)$ and $\Theta(-z)$ (i.e., the function $f$ is taken to be the same in both monolayers). Simultaneously, stretching deformation of the monolayers is equal to zero, $\mathbf{a} \equiv 0$, in the definitions of the distortion field components (see expression (14) in Sec. 3). In general, if the problem is not restricted to a weak bending deformation and/or if there are additional forces acting in the lateral direction (stretching the membrane), we may introduce $\mathbf{a}(\mathbf{r}) \neq 0$ or use two functions $f_1 \neq f_2$ in front of $\Theta(+z)$ and $\Theta(-z)$, respectively.

Results of analytic solution of the static equations in the cylindrically symmetric case are presented in Fig. 3. The lateral stress $\sigma_{rr}(r, z)$ is shown for several values of the $z$ coordinate for a bilayer with mutual interlayer slide (solid lines and dashed lines) and for a unit bilayer with forbidden slide, but of the same thickness $2h$ (lines *4*, *5*). Relaxation of lateral stresses in both monolayers is induced by mutual interlayer slide. The neutral (not stretched) surface at the interface of the membrane splits into two. Consequently, a neutral surface (with vanishing lateral stress) appears in the middle of each monolayer: at $z = +h/2$ (the upper monolayer) and at $z = -h/2$ (the lower monolayer) (line *2*). The monolayers are deformed as if they were disconnected, independent layers, but still adjusted to the same shape defined at their mutual interface inside the membrane. Therefore, the stress profiles along the $z$ axis coincide with each other in both monolayers. As a result, the stresses at the top and bottom external surfaces of the membrane ($z = \pm h$, lines *1*, *3*) decrease two times compared to the case without slide ($z = \pm h$, lines *4*, *5*). Simultaneously, as follows from (A.12), the lateral stresses at the boundary $r = R$ turn to zero through the whole depth of the membrane, $\sigma_{rr}(R, z) = 0$, corresponding to the absence of the applied external stretching forces.

## APPENDIX B

### Bilayer modes in the bulk water

To test the relevance of our approach for description of dynamical properties of a bilayer, we here rederive the dispersion relation for a membrane in the bulk water solution using our free energy functional (20) introduced in Sec. 2. Our results agree with the previous ones obtained for a membrane in the bulk fluid using the curvature elastic model [6] and the density-difference model [9].

For the surrounding bulk fluid, we search for the solution of creeping flow equations (33) (Sec. 4) satisfying the non-slip conditions at the membrane–water interface, Eqs. (34) and (35). In addition, we impose the boundary conditions for fluid velocity components $v_i$,

$$v_j(z = \pm\infty) = 0, \quad j = x, y, z, \tag{B.1}$$

which require the fluid velocity field to vanish at large distances from the membrane.

As in Sec. 4, we expand vibrations in plane waves propagating along the $x$ axis. We make a Fourier transform of free energy functional (20). The free energy density $F_s(q, \omega)$ is written as

$$F_s(q,\omega) = \frac{K_1}{2}\left\{\frac{4h^3}{3}q^4|\xi_q|^2 - \right.$$
$$\left. - 2h^2(\xi_q f_q^* - \xi_q^* f_q)q^3 i + 4h|f_q|^2 q^2\right\}. \tag{B.2}$$

The components of water velocity and pressure in the form

$$v_x = w_x(z)\exp(iqx - i\omega t), \quad v_z = w_z(z)\exp(iqx - i\omega t),$$
$$p = p_q(z)\exp(iqx - i\omega t)$$

are substituted in Fourier-transformed creeping flow equations (41) (see Sec. 4). The solutions of differential equations (41) satisfying boundary conditions (B.1), with the normal velocity continuous at $z = 0$ and also obeying the condition of zero lateral stretching force acting on the membrane (Eq. (32) in Sec. 4) are given by

$$p_q = \begin{cases} -2\eta_w C_1 e^{-qz}, & z > 0, \\ 2\eta_w C_1 e^{qz}, & z < 0, \end{cases} \tag{B.3}$$

$$w_z = \begin{cases} [-C_1 z + C_3]e^{-qz}, & z > 0, \\ [C_1 z + C_3]e^{qz}, & z < 0, \end{cases} \tag{B.4}$$

$$w_x = \begin{cases} \left[C_1 z - C_3 - \dfrac{C_1}{q}\right] ie^{-qz}, & z > 0, \\ \left[C_1 z + C_3 + \dfrac{C_1}{q}\right] ie^{qz}, & z < 0, \end{cases} \tag{B.5}$$

where the constants $C_2$ and $C_4$, which are present in Eqs. (42)–(44), turn to zero due to boundary conditions (B.1).

The unknown coefficients $C_1$ and $C_3$ are determined from non-slip conditions (34) and (35). Then, we substitute solutions (B.3)–(B.5) in Fourier transforms of force balance equations (30) and (31) and obtain an algebraic system of two linear homogeneous equations for the components $\xi_q$ and $f_q$,

$$\xi_q \left[-\frac{2h^3}{3} K_1 q^4 + 4\eta_w i q \omega\right] + f_q \left[-K_1 h^2 i q^3\right] = 0, \tag{B.6}$$

$$\xi_q(-h^2 K_1 q^3 i) + \\ + f_q \left(2K_1 h q^2 - 2i\omega(\eta_m h q^2 + 2\eta_w q + b_s)\right) = 0. \tag{B.7}$$

Equating the determinant of this system to zero, we obtain a quadratic equation for $\omega(q)$, which results in two branches $\omega_1(q)$ and $\omega_2(q)$. There are three hydrodynamic regimes,

$$q \ll q_1, \quad q_1 \ll q \ll q_2, \quad q_2 \ll q,$$

separated by crossover wave vectors $q_1$ and $q_2$ [9]:

$$q_1 = \frac{\eta_w}{b_s h^2}, \quad q_2 = \sqrt{\frac{b_s}{\eta_m h}}\,. \tag{B.8}$$

For long wavelengths, $q \ll q_1$, the dispersion relations are given by

$$\omega_1^B = -iq^3 \frac{K_1 h^3}{24\eta_w} \approx -iq^3 \frac{K_b}{\eta_w}, \tag{B.9}$$

$$\omega_2^B = -iq^2 \frac{K_1 h}{b_s} \approx -iq^2 \frac{K_A}{b_s}, \tag{B.10}$$

which describe respectively the hydrodynamically damped bending mode $\omega_1^B(q)$ and the intermonolayer slipping mode $\omega_2^B(q)$ damped by viscous drag at the membrane mid-plane. Here, the superscript «$B$» is introduced to label membrane modes in the bulk fluid.

For wave vectors in the interval $q_1 \ll q \ll q_2$, the bending and slipping modes mix [9],

$$\omega_1^B = -iq^2 \frac{K_1 h}{4b_s} \approx -iq^2 \frac{K_A}{b_s}, \tag{B.11}$$

$$\omega_2^B = -iq^3 \frac{K_1 h^3}{6\eta_w} \approx -iq^3 \frac{K_b}{\eta_w}\,. \tag{B.12}$$

The branch $\omega_2^B(q)$ now corresponds to the bending mode damped by viscous losses in the surrounding fluid, and the branch $\omega_1^B(q)$ describes the damping of the slipping mode. The elastic moduli in (B.11) and (B.12) differ in general from those in (B.9) and (B.10), because high-frequency (bending) fluctuations occur at nonrelaxed monolayer surface densities [9].

In the short-wavelength limit, $q \gg q_2$, we obtain

$$\omega_1^B = -i \frac{K_1}{4\eta_m}\,, \tag{B.13}$$

$$\omega_2^B = -iq^3 \frac{K_1 h^3}{6\eta_w} \approx -iq^3 \frac{K_b}{\eta_w}\,. \tag{B.14}$$

The $\omega_1^B(q)$ mode is driven by the (high-frequency) effective rigidity $K_1$ and is damped by the monolayer surface viscosity $\eta_m$. Effective rigidity is induced by dynamic coupling of monolayers [3]. Monolayer surface viscosity overwhelms interlayer drag and becomes the main source of dissipation.

## REFERENCES


1. A. Ben-Shaul, in *Structure and Dynamics of Membranes*, ed. by R. Lipowsky and E. Sackmann, Elsevier Science (1995), Ch. 7.
2. U. Seifert and R. Lipowsky, ibid, Ch. 8.
3. A. Yeung and E. Evans, J. de Phys. II **5**, 1501 (1995).
4. E. I. Kats and V. V. Lebedev, *Fluctuational Effects in the Dynamics of Liquid Crystals*, Springer-Verlag, New York (1993).
5. W. Helfrich, Z. Naturforsch **28**, 693 (1973).
6. F. Brochard and J. F. Lennon, J. Phys. **36**, 1035 (1975).
7. W. Helfrich, Z. Naturforsch **33**, 305 (1977).

**8**. E. Evans and A. Yeung, Lipids Chem. Phys. **73**, 39 (1994).

**9**. U. Seifert and S. A. Langer, Europhys. Lett. **23**, 71 (1993).

**10**. M. Kraus and U. Seifert, J. de Phys. II **4**, 1117 (1994).

**11**. U. Seifert, Phys. Rev. E **49**, 3124 (1994).

**12**. F. C. MacKintosh, Phys. Rev. E **50**, 2891 (1994).

**13**. L. D. Landau and E. M. Lifshitz, *Theory of Elasticity. Theoretical Physics*, Pergamon Press, New York (1980), Vol. 7.

**14**. H. Kleinert, *Gauge Fields in Condensed Matter. Stresses and Defects*, World Scientific Publishing, Singapore (1989), Vol. 2.

**15**. S. A. Safran, *Statistical Thermodynamics of Surfaces, Interfaces and Membranes*, Perseus Pr. Publisher, New York (1994).

**16**. E. I. Kats, V. V. Lebedev, and S. V. Malinin, Zh. Eksp. Teor. Fiz. **113**, 2096 (1998).